DOI: 10.13009/EUCASS2017-321

Reconfiguration control method for non-redundant actuator faults on UAV

Adèle Boche⋆ and Jean-Loup Farges⋆ and Henry De Plinval⋆
⋆ONERA - The French Aerospace Lab
2 avenue Edouard Belin, F-31055 Toulouse, France
name.surname@onera.fr

Abstract

In this article, an indirect continuous and discrete Fault Tolerant Control scheme is applied to the longitudinal dynamics of a fixed-wing UAV. To address the problem raised by a possible engine fault, the FTC method is adapted to non-redundant actuator faults by considering signatures on residuals, designing discounted cost optimal controllers, using rolling horizon techniques and considering actuator dynamics in the state equation. The efficiency of the proposed approach is demonstrated on a scenario involving thrust and elevon faults during a landing procedure.

1. Introduction

Because safety and reliability are more and more important for Unmanned Aerial Vehicles (UAVs), many works have been done on Fault Tolerant Control (FTC) to improve them.[12] There are two types of FTC methods, the passive one and the active one. Passive methods are designed to be robust against faults without the need for change in the control scheme, whereas active methods react by reconfiguring their control action.[5] The most common active FTC method is the indirect method where the action of control is reconfigured considering the output of a fault detection and isolation module. The Fault Detection and Isolation (FDI) step is generally based on residuals which are used for decision making.[4] Several methods have been developed for the reconfiguration. An approach uses eigenstructure assignment technique for computing on-line new feedback and feedforward gains.[11] However, it only covers loss of effectiveness actuator faults, that is when the actuator only responds partially to the control order, and does not cover other faults, as when the actuator is stuck at a given value. A common approach is to use adaptive controller and to adapt it indirectly to fault parameters.[4] Another common approach is to use multiple models.[10] A bank of parallel models is used to describe the system under nominal mode and degraded modes. A corresponding controller is designed for each of these models. Recently, an approach based on continuous and discrete models of faults has been proposed.[3] It considers only one model with a bank of controllers associated to nominal and faulty conditions. This model covers both nominal and faulty conditions, so that one is able to keep track of fault probabilities. Based on this approach, improved and applied to longitudinal control of UAV with redundant actuators,[2] the purpose of the work presented here is to investigate the applicability of the reconfiguration framework to multiple actuator faults addressing the case where actuators are not redundant. In particular, the possible failure of the UAV engine is considered and leads to four contributions; firstly fault signatures on residuals are used to activate signals allowing an identification of relevant fault parameters, secondly a controller is designed by the Linear Quadratic (LQR) method considering a discounted cost and a bias in the state equation, thirdly a model predictive control framework is used to take into account the possible cost of switching dynamics, finally actuator dynamics are taken into account in the state equation. This article is organised as follows. In Section 2, the addressed problem is described and the reconfiguration principle is provided. In Section 3, the technique used for signal activation is described. In section 4, the reconfiguration method is improved. A controller for non-redundant actuator faults is developed and a new controller selection method is described. Finally, in Section 5, simulation results for a scenario presenting an engine fault are shown.

DOI: 10.13009/EUCASS2017-321

2. FRAMEWORK

2.1 Addressed problem

The considered UAV is a fixed-wing UAV with back engine, the "L'avion jaune" Altimum 4 which has been modelled.[6] The problem addressed is to control the longitudinal motion of the UAV in order to continue to follow its reference trajectory despite the possible fault of one of the actuators. The model of this UAV has three control variables; the thrust command, which is non-redundant, and the left and right elevons commands, which are redundants. Inspired from the FAA advisory circular 25.1309-1 for manned aircraft that states that "Failures of any system should be assumed for any given flight regardless of probability and such failure 'should not prevent continued safe flight and landing' or otherwise significantly reduce safety", the reconfiguration problem takes into account the fact that each actuator could become faulty. Moreover, both the locking and the loss of effectiveness of actuators are considered.

2.2 An indirect FTC method

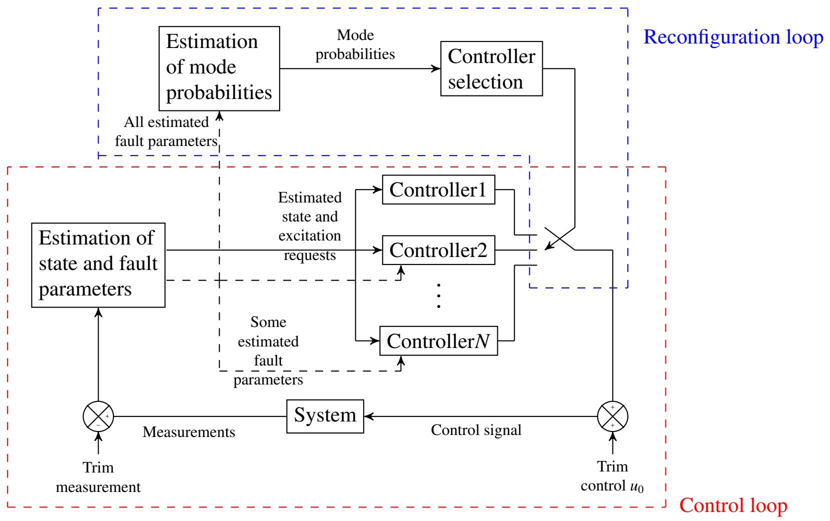

Figure 1: Overview of the FTC method

The FTC method presented in Fig. 1 takes advantages from reconfiguration, through estimation of mode probabilities and controller selection using a discrete model, and from indirect adaptive control, through estimation of fault parameters and controllers taking into account some fault parameters using a continuous model. Note that the method have two closed loop, the reconfiguration one and the control one. The two loops have different sampling times, the control loop have a sampling time Δt and the reconfiguration loop have a sampling time Δt_{Reconf} which is longer than Δt.

Aspects represented by continuous dynamics are the system behaviour and its controllers, but also an indicator of performance and an estimation scheme. Other features are represented by discrete state dynamics; the system modes and their transition probabilities, but also a decision making framework -based on rewards computed from the indicator of performance- to chose the best suitable controller for the continuous model.

In a previous study,[2] the FTC method has been applied only to redundant actuator faults. However, the thrust command is not redundant with right and left elevon commands. This remark means that, contrary to the case where two actuators have the same effect on the UAV, in this case, the engine effect on the system state is completely different to the actuators effects. In this article, in order to address the problem raised by a possible engine fault, the FTC method is applied not only for redundant actuator faults, but also for non-redundant actuator faults. For the FTC method, it implies several improvements which are described thereafter.

DOI: 10.13009/EUCASS2017-321

2.3 Model of the system

2.3.1 Fault free model

A linearised model is used for the development of software components based on continuous dynamics. For a UAV longitudinal model linearised for a typical flight condition -with a given air speed and a given slope-, the system can be described by the following discretised equations:

$$\begin{aligned} \boldsymbol{x}_{k+1} &= A\boldsymbol{x}_k + B\boldsymbol{u}_k + \boldsymbol{w}_k{}^x \\ z_k &= C\boldsymbol{x}_k + \boldsymbol{v}_k \end{aligned} \tag{1}$$

Where $\boldsymbol{x}_k \in \mathbb{R}^n$ corresponds to the states: horizontal and vertical velocity, pitch rate, horizontal and vertical position, pitch angle, thrust, left elevon and right elevon; $\boldsymbol{u}_k \in \mathbb{R}^p$ corresponds to the desired control inputs: thrust command, left elevon command and right elevon command; $\boldsymbol{w}_k \in \mathbb{R}^n$ corresponds to modelling errors; $\boldsymbol{v}_k \in \mathbb{R}^m$ corresponds to the measurement noise; $z_k \in \mathbb{R}^m$ corresponds to the outputs: the six first outputs are the six first states, the others are: longitudinal part of load factor, vertical part of load factor, angle of attack, slope, calibrated air speed, and air speed.
The characterization of actuator redundancies is based on the following definition.

Definition Assume the system is described by equation 1. Let us define the associated $m \times p$ transfer function matrix $G(z)$. Two actuators, i.e two inputs u_k^i and u_k^j are said to be redundants if the i^{th} and the j^{th} columns of the transfer function matrix $G(z)$ are linearly dependant, i.e $rank(\begin{bmatrix} G_{(:,i)}(z) & G_{(:,j)}(z) \end{bmatrix}) = 1$

The concept of redundant actuators is defined by dependant columns of the transfer function matrix $G(z)$. Here, the columns of $G(z)$ associated to the right and left elevon commands are the same. Thus, the right and the left elevon commands are redundants. However, the thrust command and the left or right elevon command are non-redundant.

2.4 Faulty actuator models

In equation 1, the actuators are modelled with first orders. The time constant from an elevon command to the associated elevon state is small with respect to vehicle dynamics, while the time constant from the engine command to the engine state is of the same magnitude than the quickest vehicle dynamic. However the fault of an actuator is always considered occurring at the level of the command, leading to the definition of the effect e_k^i of the i^th actuator at time k by:

$$e_k^i = b_{0k}^i + (1 - b_{1k}^i)u_k^i - b_{1k}^i u_0^i \tag{2}$$

Where $\boldsymbol{u}_0$ is the trim control input; b_{0k}^i and b_{1k}^i are fault parameters.
Note that the parameters of $\boldsymbol{b_0}$ are biases, so that they cannot be differentiated for redundant actuators, i.e. for the elevons. However, the knowledge of $\boldsymbol{b_1}$ is sufficient to detect which actuator is faulty and only the sum of the values of $\boldsymbol{b_0}$ for redundant actuators will be considered and estimated thereafter. Thus, the dimension of $\boldsymbol{b_0}$ is two while the dimension of $\boldsymbol{b_1}$ is three. The values of the parameters $\boldsymbol{b_0}$ and $\boldsymbol{b_1}$ and their brutal changes are unknown. Thus, their behaviours are modelled as random walks:

$$\boldsymbol{b_0}_{k+1} = \boldsymbol{b_0}_k + \boldsymbol{w}_k{}^{b_0} \qquad \boldsymbol{b_1}_{k+1} = \boldsymbol{b_1}_k + \boldsymbol{w}_k{}^{b_1} \tag{3}$$

Note that the control input $\boldsymbol{u}_k$ is limited between $\boldsymbol{u_{min}} = \underline{\boldsymbol{u}}$ and $\boldsymbol{u_{max}} = \overline{\boldsymbol{u}}$. Thus, the fault parameter $\boldsymbol{b_0}_k$ is also limited between $\underline{\boldsymbol{u}}$ and $\overline{\boldsymbol{u}}$. The fault parameter $\boldsymbol{b_1}_k$ correspond to an effectiveness thus it is limited in $[0, 1]^3$.

2.4.1 Fault Model

For a UAV longitudinal model linearised for a typical flight condition, the system taking into account actuator faults can be obtained by substituting in equation 1 $\boldsymbol{u}_k$ by $\boldsymbol{e}_k$ given by equation 2:[3]

$$\begin{aligned} \boldsymbol{x}_{k+1} &= A\boldsymbol{x}_k + B\boldsymbol{u}_k + B\boldsymbol{b_0}_k + D(\boldsymbol{u}_k)\boldsymbol{b_1}_k + \boldsymbol{w}_k{}^x \\ z_k &= C\boldsymbol{x}_k + \boldsymbol{v}_k \end{aligned} \tag{4}$$

with $D(\boldsymbol{u}_k) = B.diag\{-u_k^1 - u_0^1, -u_k^2 - u_0^2, -u_k^3 - u_0^3\}$.

DOI: 10.13009/EUCASS2017-321

3. ESTIMATION

The state of the system and the fault parameters are estimated using a Kalman filter. This filter is modified in order to take into account specific features of faults parameters; bounded values, step change and low observability. Mode probabilities are estimated using the values of the fault parameters.

3.1 Estimation of state and fault parameters

3.1.1 A Kalman filter with time dependent state matrix

To estimate the state $\boldsymbol{x}$ and the parameters $\boldsymbol{b_0}$ and $\boldsymbol{b_1}$, an augmented system is considered, which includes the system natural state together with the fault parameters $\boldsymbol{X}_k^T = \begin{bmatrix} \boldsymbol{x}_k^T & \boldsymbol{b_0}_k^T & \boldsymbol{b_1}_k^T \end{bmatrix}^T$. Then a Kalman filter is applied to the resulting augmented system, which may be described by:

$$\begin{aligned} \boldsymbol{X}_{k+1} &= A_k^{aug}\boldsymbol{X}_k + B^{aug}\boldsymbol{u}_k + \boldsymbol{W}_k^{aug} \\ z_k &= C^{aug}\boldsymbol{X}_k + \boldsymbol{v}_k \end{aligned} \tag{5}$$

with $A_k^{aug} = \begin{bmatrix} A & B & D(\boldsymbol{u}_k) \\ 0_{2,9} & I_2 & 0_{2,3} \\ 0_{3,9} & 0_{3,2} & I_3 \end{bmatrix}$, $B^{aug} = \begin{bmatrix} B^T & 0_{3,5} \end{bmatrix}^T$, $C^{aug} = \begin{bmatrix} C & 0_{12,5} \end{bmatrix}$, and $\boldsymbol{W}_k^{aug} = \begin{bmatrix} \boldsymbol{w}_k{}^{xT} & \boldsymbol{w}_k{}^{b_0T} & \boldsymbol{w}_k{}^{b_1T} \end{bmatrix}^T$

Note that $\boldsymbol{W}_k^{aug}$ is assumed to be a zero mean Gaussian white noise with covariance Q, and $\boldsymbol{v}_k$ is assumed to be a zero mean Gaussian white noise with covariance R.

In the estimation algorithm, the matrix covariance $P_{k+1|k}$ is reset at relevant times in order to capture the possible faults.

3.2 Adaptation of the filter

3.2.1 Projection of constrained states

The fault parameters are restricted. $\boldsymbol{b_0}_k$ is restricted following the limits of $\boldsymbol{u}_k$, and $\boldsymbol{b_1}_k$ is limited in $[0, 1]$[3].

Assume at each time step k, $\boldsymbol{X}_k$ is subject to the following inequality:

$$D_k\boldsymbol{X} \leq \boldsymbol{d} \tag{6}$$

To solve this inequality the active set method is used.[9] At each time step k, the inequality 6 is tested. Thus, for each scalar constraint in equation 6 there are two scenarios:

- If the inequality is passed, nothing is done,
- If the inequality is not passed, an equality constraint is applied: $D_{i,:}\boldsymbol{X}_k = d_i$

This equality constrained problem can be solved by projection.[9] The optimization problem to be solved is the following:

$$\begin{aligned} \min_{\widehat{\boldsymbol{X}}_k^c} \quad & (\widehat{\boldsymbol{X}}_k^c - \widehat{\boldsymbol{X}}_k^{nc})^T(\widehat{\boldsymbol{X}}_k^c - \widehat{\boldsymbol{X}}_k^{nc}) \\ s.t. \quad & E_k\widehat{\boldsymbol{X}}_k^c = e_k \end{aligned} \tag{7}$$

where $\widehat{\boldsymbol{X}}_k^c$ is the estimation of the constrained augmented state and $\widehat{\boldsymbol{X}}_k^{nc}$ is the estimation of the non-constrained augmented state, $E_k = \begin{bmatrix} D_{i_1,:}^T & \cdots & D_{i_n,:}^T \end{bmatrix}^T$ and $e_k = \begin{bmatrix} d_{i_1} & \cdots & d_{i_n} \end{bmatrix}^T$ where $i_1, ..., i_n$ are the indexes of the scalar constraints for which inequality constraints are not passed.

The solution of 7 is synthesized by the following equations:

$$\begin{aligned} \widehat{\boldsymbol{X}}_k^c &= \widehat{\boldsymbol{X}}_k^{nc} + L_k(e_k - E_k\widehat{\boldsymbol{X}}_k^{nc}) \\ L_k &= E_k^T(E_kE_k^T)^{-1} \end{aligned} \tag{8}$$

These constraint equations are coupled with the augmented Kalman filter with a semi-closed loop, as shown on the Fig 2. That is mean that the non-constrained covariance P_k^{nc} and the constrained state $\widehat{\boldsymbol{X}}_k^c$ are used for the Kalman filter.

The adjustment of the covariance matrix would reduce its values, and would focus the filter solution too quickly. Thus a full closed loop is not suitable for the Kalman filter. For the rest of this article, $P_k^{nc} = P_k^c = P_k$.

DOI: 10.13009/EUCASS2017-321

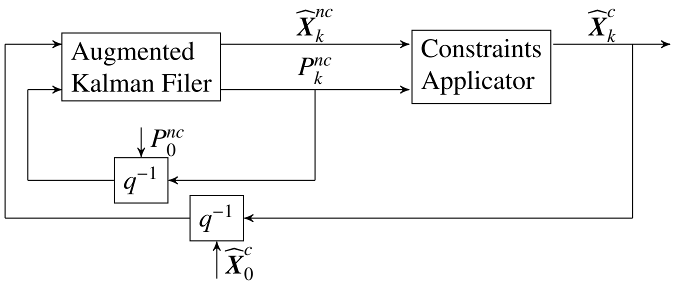

Figure 2: Semi-closed loop

3.2.2 Reset of the relevant part of the covariance matrix

The fault parameters b_0 and b_1 are modelled as random walks, thus a sudden change cannot be detected with this model. A method often used in FDI is the residual generation method. For this FTC method, the step change of fault parameters is taken into account by managing the 3 residuals defined as follows:

$$r_q = \mu_3(C_{3,:}P_{k+1|k}C_{3,:}{}^T + R_{33})^{-1}\mu_3 \tag{9}$$
$$r_{n_x} = \mu_7(C_{7,:}P_{k+1|k}C_{7,:}{}^T + R_{77})^{-1}\mu_7 \tag{10}$$
$$r_{n_z} = \mu_8(C_{8,:}P_{k+1|k}C_{8,:}{}^T + R_{88})^{-1}\mu_8 \tag{11}$$

Where μ_3, μ_7, and μ_8 corresponds to the innovation of the pitch rate, the longitudinal part of the load factor, and the vertical part of the load factor.
Only the measurements of the longitudinal and vertical part of the load factor and the pitch rate are considered because simple flight dynamics considerations indicate that an engine fault impacts first the acceleration and thus the longitudinal part of the load factor, and an elevon fault impacts first the pitch rate and the vertical part of the load factor. Faulty actuators -thrust and elevons- have different specific signatures on the residuals r_{n_x}, r_q and r_{n_z} (see Table 1).

Table 1: Fault signatures on residuals

Reset of the covariance for:	Signature
δ_x	$(r_{n_x} \geqslant t_{n_x} \wedge r_q < t_q) \vee (r_{n_x} \geqslant t_{n_x} \wedge r_q \geqslant t_q \wedge r_{n_z} \geqslant r_{n_x})$
δ_r and δ_l	$(r_{n_x} < t_{n_x} \wedge r_q \geqslant t_q) \vee (r_{n_x} \geqslant t_{n_x} \wedge r_q \geqslant t_q \wedge r_{n_z} < r_{n_x})$

In Table 1, t_q and t_{n_x} are given thresholds, used to suspect that a fault has occurred.
When one of the residuals exceeds the threshold, it suggests a sudden change of the fault parameters -that is not taken into account in the model-, and thus a possible switching of mode.
Once a change is suggested, the matrix covariance $P_{k+1|k}$ is reset following the signature. If the signature of thrust, respectively elevons, is recognized, the covariance associated to the fault parameters of the thrust, respectively elevons, are reset to zero and the variances are reset to $((\overline{u}_1 - \underline{u}_1)/t_{n_x})^2$, respectively $((\overline{u}_2 - \underline{u}_2)/t_q)^2$, for the associated parameters of $\boldsymbol{b_0}$ and to $1/(t_{n_x})^2$, respectively $1/(t_q)^2$, for the associated parameters of $\boldsymbol{b_1}$.
Only the covariances corresponding to the fault parameters are reset. No information is known on fault parameters when a signature is recognized, and the augmentation in the covariance $P_{k+1|k}$ is designed to capture it. The variances are reset in order to take into considerations all the possible values for b_0 and b_1.
Note that $t_q = 25$ and $t_{n_x} = 25$. This choice has been verified with a Monte Carlo method.
The Table 2 shows simulation results for left elevon faults. For all the simulations, the thrust and the right elevon are nominal, and the left elevon is locked or less effective. When the elevon recover its effectiveness, in 0.9% of the simulations there is a false alarm suspecting that the thrust is faulty. In some cases, there is no reset when the elevon is less efficient. This corresponds to small value of b_1, in this case, there is no need to reset the covariance because the random walk could modelled it.
The Table 3 shows simulation results for engine faults. For all the simulations, the elevons are nominal, and the engine is locked or less effective. In some cases, there is no reset when the engine is locked. This is for a control value close to the trim value. In this case, there is no change in the system and it cannot be detected. In some cases, there is no

DOI: 10.13009/EUCASS2017-321

Table 2: Monte Carlo

	Number of simulation	Inappropriate reset	No reset
Elevon nominal → Elevon locked	1000	0	0
Elevon locked → Elevon nominal	1000	17 for the thrust	0
Elevon nominal → Elevon less efficient	1000	0	74 ($b_1 < 0.1$)
Elevon less efficient → Elevon nominal	1000	1 for the thrust	83 ($b_1 < 0.1$)

Table 3: Monte Carlo

	Number of simulation	Inappropriate reset	No reset
Engine nominal → Engine locked	1000	0	70 ($b_0 \sim u_0$)
Engine locked → Engine nominal	1000	0	0
Engine nominal → Engine less efficient	1000	0	165 ($b_1 < 0.2$)
Engine less efficient → Engine nominal	1000	0	179 ($b_1 < 0.2$)

reset when the engine is less efficient. This corresponds to small value of b_1, in this case, there is no need to reset the covariance because the random walk could modelled it.

3.2.3 Observability of fault parameters

A reliable estimation is needed for the detection of the faults. It would not be possible to estimate $\boldsymbol{b_0}$ and $\boldsymbol{b_1}$ properly if the longitudinal mode is not sufficiently excited. Thus, when the estimation of state and fault parameters resets the covariance $P_{k+1|k}$, at the same time, it sends to the controllers an excitation request indicating whether elevons or engine shall be excited.

3.3 Estimation of mode probabilities

3.3.1 Modes and transitions between modes

The proposed framework considers only single faults at a time. It is assumed that three actuators can become faulty. Thus, based on the framework defined in,[3] there is four modes; a nominal mode, a faulty mode for the engine, a faulty mode for left elevon and a faulty mode for right elevon.
The transition probabilities between these modes are stationary and given by the matrix T_M:

$$T_M = \begin{bmatrix} p(m_0|m_0) & \cdots & p(m_0|m_3) \\ \vdots & \ddots & \vdots \\ p(m_3|m_0) & \cdots & p(m_3|m_3) \end{bmatrix}$$

3.3.2 Observations

The observation is based on the information of the continuous process provided by the estimation scheme: $\omega = \{\widehat{\boldsymbol{b_0}}_k, \widehat{\boldsymbol{b_1}}_k\}$. Assuming $p(\boldsymbol{b_0}, \boldsymbol{b_1}|\omega) = p(\omega|\boldsymbol{b_0}, \boldsymbol{b_1})$, the observation probability is given by integrating this quantity over the domain corresponding to each mode, namely:

$$p(\omega|m) = \int f_m(\boldsymbol{b_0}, \boldsymbol{b_1}) p(\omega|\boldsymbol{b_0}, \boldsymbol{b_1}) \mathrm{d}\boldsymbol{b_0} \mathrm{d}\boldsymbol{b_1} \tag{12}$$

where $f_m(\boldsymbol{b_0}, \boldsymbol{b_1})$ depend on the mode.
It is assumed that the fault parameters are independents. Assumptions are made on the distribution of the parameters of $\boldsymbol{b_0}$ and $\boldsymbol{b_1}$ for each mode.[3]

3.3.3 Belief update

The probabilities of modes are gathered in a vector b. At each step the vector b is predicted:

$$b_{n+1|n} = T_M b_{n|n} \tag{13}$$

DOI: 10.13009/EUCASS2017-321

Where T_M is the matrix of transition probabilities.
Then, the mode probabilities are updated from the observation ω. The Bayes rule is used:

$$b_{n+1|n+1}(m) = b_{n+1|n}(m)\frac{p(\omega|m)}{\sum_{m'} b_{n+1|n}(m')p(\omega|m')} \tag{14}$$

The detection of a mode is based on these mode probabilities.
Note that the whole mechanism is designed in order to be sensitive to faults and robust in case of absence of fault. The signature of the residuals leads to suspect some kind of faults. Based on this suspicion, some specific parts of the covariance matrix are reset and some specific excitation signals are sent allowing an estimation of fault parameters. The updated fault parameters change the mode probabilities. This mechanism is proposed because false alarms can appear with the signature of the residuals.

4. RECONFIGURATION

4.1 Structure of controllers

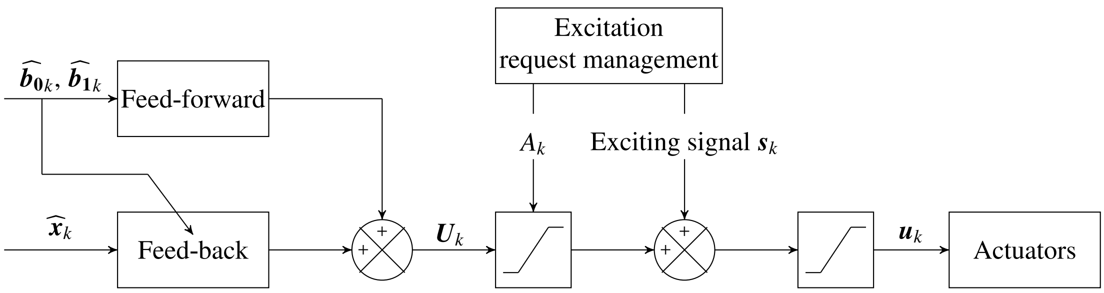

Figure 3: Controller and saturation

When an excitation on the system is requested, a specific signal is added to the feed-back and feed-forward signals of the controller as shown on the Fig. 3. The control signal is as follows:

$$u_k^i = f(U_k^i, s_k^i, A_k) = \min\{\overline{u}^i, \max\{\underline{u}^i, \min\{\overline{u}^i - A_k, \max\{\underline{u}^i + A_k, U_k^i\}\} + s_k^i\}\} \tag{15}$$

Where A_k corresponds to the amplitude A of the exciting signal s_k^i when it is present and zero otherwise. This highest saturation rate is done in order to let pass the exciting signal in all situations.
Most of the time, the system do not request an excitation. In this case, s_k^i is null and the control signal is as follows:

$$u_k^i = \min\{\overline{u}^i, \max\{\underline{u}^i, U_k^i\}\} \tag{16}$$

4.1.1 Behaviour on excitation request

For the engine, the thrust input manoeuvre usually used is a doublet.[8] This signal excites a band at high frequency. This is a series of two alternating step inputs (see Fig. 4). The amplitude A should not be too high in order to have a low impact on the airspeed of the UAV. The period ΔT have to take into consideration the time constant of the engine.
For the elevons, opposite signals should be sent to left and right actuators to provide excitation. The objective of this signal is to be able to distinguish b_1^1 from b_1^2, so that the global associated control input, which is the sum of them, is null; it has no effect on the trajectory -it is sent with a positive sign on δ_l and with a negative sign on δ_r- but only on the observability. The 3211 input signal is preferred because it excite a broader dynamic spectrum of the system within a short period.[8] This is a series of alternating step inputs, the duration of which satisfies the ratio 3, 2, 1, 1.
The 3211 signals, respectively the doublet signal, is sent when the covariances associated to the fault parameters of the elevons, respectively the engine, are reset. Moreover, three seconds after, if the fault parameter b_1^1 associated to the thrust command is greater than 0.7, another doublet signal is sent.

DOI: 10.13009/EUCASS2017-321

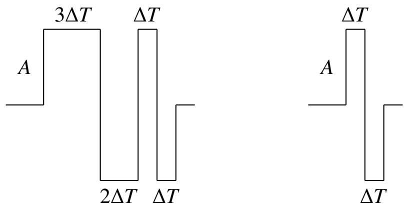

Figure 4: On the left, 3211 control input, on the right, doublet control input

4.1.2 Performance indicator

For each mode an associated controller is designed. The desired effective control $\boldsymbol{e}_k$ is:

$$\boldsymbol{e}_k = -K\widehat{\boldsymbol{x}}_k \tag{17}$$

The gain K is calculated using the Linear Quadratic Regulator (LQR) method by minimizing the performance index defined as J_0^∞, with:

$$J_k^{k''} = \sum_{k'=k}^{k'=k''} \alpha^{k'} (\boldsymbol{x}_{k'}{}^T Q_{lqr} \boldsymbol{x}_{k'} + \boldsymbol{u}_{k'}{}^T R_{lqr} \boldsymbol{u}_{k'}) \tag{18}$$

It corresponds to a mixed state-control criterion with a discounted factor α.
A discounted factor is used because if the engine is locked at a position, the sum of elementary costs may not be finite inducing a problem of convergence while solving the Riccati equation. When the engine is locked, the pair (A, B) is not controllable any more but it is still stabilizable. The eigenvalues are in the unit circle, however, two eigenvalues are on it. Thus, a discounted cost is needed in the LQR method to enforce the convergence of the Riccati equation.[1] For a discounted LQR, the gain K is calculated with the classical Riccati equation applied to the pair ($\sqrt{\alpha}A$, $\sqrt{\alpha}B$).
The aims is to follow the trajectory and so the slope γ. The horizontal position x and the vertical position z are linked by the following equation: $z = tan(\gamma)x$. Thus, Q_{lqr} is chosen as follows: $Q_{lqr} = diag\{0, 0, 0, tan^2(\gamma), 1, 0, 0, 0, 0\}$.

4.1.3 Nominal controller

For the nominal mode, the controller is as follows.

$$\boldsymbol{u}_k = \left[f(-K_{1.}\widehat{\boldsymbol{x}}_k, S_{doublet}, A_k) \qquad f(-K_{2.}\widehat{\boldsymbol{x}}_k, S_{3211}, A_k) \qquad f(-K_{2.}\widehat{\boldsymbol{x}}_k, -S_{3211}, A_k) \right]^T \tag{19}$$

Where $K^T = [K_{1.}^T K_{2.}^T K_{2.}^T]$, S_{3211} is a 3211 signal input which is added when an elevon faults is suggested and $S_{doublet}$ is a doublet signal which is added when an engine fault is suggested.

4.1.4 Faulty controller for redundant actuator

One controller is designed for the two redundant actuators. This controller is designed to improve performance for both locking case and loss of effectiveness case and for both left and right elevons. Even if the same controller is used for the fault of right and left elevons, it is interesting to keep two different modes for the elevons in order to know which of them is faulty. Thus, there is four modes $\{m_0, m_1, m_2, m_3\}$ and three controllers $\{c_0, c_1, c_2\}$.
The left and right actuators have the same effect and it is not desired to compensate the effect of the faulty actuator using thrust command.
On the one hand, having the same feedback than in the absence of fault implies:

$$e_k^2 + e_k^3 = -2K_{2.}\widehat{\boldsymbol{x}}_k \tag{20}$$

On the other hand, the control implies:

$$e_k^2 + e_k^3 = b_0^2 + (1 - b_1^2)u_k^2 - b_1^2 u_0^2 + (1 - b_1^3)u_k^3 - b_1^3 u_0^3 \tag{21}$$

Combining (20) and (21), Φ is defined as:

$$\Phi(u_k^2, u_k^3) = 2K_{2.}\widehat{\boldsymbol{x}}_k + b_0^2 + (1 - b_1^2)u_k^2 - b_1^2 u_0^2 + (1 - b_1^3)u_k^3 - b_1^3 u_0^3 \tag{22}$$

DOI: 10.13009/EUCASS2017-321

In defining the control in faulty condition, the goal is to minimize the control action. However, the S_{3211} signal shall still be added to it -still with a null global effect- to maintain observability of the fault. Thus, the control signal is as follows:

$$\boldsymbol{u}_k = \begin{bmatrix} f(-K_{1.}\widehat{\boldsymbol{x}}_k, S_{doublet}, A_k) & f(U_k^2, (1-\widehat{b_1^3})S_{3211}, A_k) & f(U_k^3, -(1-\widehat{b_1^2})S_{3211}, A_k) \end{bmatrix}^T \tag{23}$$

And the optimization problem to be solved is:

$$\begin{array}{c} \min_{U_k^2, U_k^3} \frac{1}{2}((U_k^2)^2 + (U_k^3)^2) \\ s.t. \qquad \Phi(u_k^2, u_k^3) = 0 \end{array} \tag{24}$$

The command optimizing (24) is then:

$$U_k^2 = -\lambda(1-\widehat{b_1^2}) \qquad U_k^3 = -\lambda(1-\widehat{b_1^3}) \tag{25}$$

Where λ is equal to: $\lambda = (\widehat{b_0^2} - \widehat{b_1^2}u_0^2 - \widehat{b_1^3}u_0^3 + 2K_{2.}\widehat{\boldsymbol{x}}_k)/((1-\widehat{b_1^2})^2 + (1-\widehat{b_1^3})^2)$

4.1.5 Faulty controllers for non-redundant actuator

By definition, in the faulty case, the thrust effective control, e.g. the 1^{st} one, has the following form: $b_0^1 + (1-b_1^1)u_k^1 - b_1^1 u_0^1$, while the others are in nominal mode.
Thus, $\boldsymbol{x}_{k+1} = A\boldsymbol{x}_k + \begin{bmatrix}(1-b_1^1)B_{.,1} & B_{.,2} & B_{.,3}\end{bmatrix}\boldsymbol{u}_k + B_{.,1}(b_0^1 - b_1^1 u_0^1) + \boldsymbol{w}_k$
The term $B_{.,1}(b_0^1 - b_1^1 u_0^1)$ is not considered in the theory of discounted LQR. In the following theorem, it is shown that this additional term implies adding a signal $\boldsymbol{v}_k$ to the feedback.

Theorem 4.1 (Discounted LQR method with an additional term) *Let the plant to be controlled be described by the following linear equation:*

$$\boldsymbol{x}_{k+1} = A\boldsymbol{x}_k + E\boldsymbol{u}_k + F \tag{26}$$

The associated performance index is the discounted quadratic cost function:

$$J_0^\infty = \sum_{k=0}^{k=\infty} \alpha^k (\boldsymbol{x}_k{}^T Q \boldsymbol{x}_k + \boldsymbol{u}_k{}^T R \boldsymbol{u}_k) \tag{27}$$

The command optimizing the performance index is the following:

$$\boldsymbol{u}_k = -\alpha(R + \alpha E^T P E)^{-1} E^T P A \boldsymbol{x}_k - \alpha(R + \alpha E^T P E)^{-1} E^T [PF - \boldsymbol{v}] \tag{28}$$

with: $P = Q + \alpha A^T[P - \alpha PE(\alpha E^T PE + R)^{-1}E^T P]A$ *and* $\boldsymbol{v} = \alpha A^T (Id + \alpha PER^{-1}E^T)^{-1}(\boldsymbol{v} - PF)$

Proof The associated Hamiltonian function is:

$$H_k = \frac{1}{2}\alpha^k(\boldsymbol{x}_k^T Q \boldsymbol{x}_k + \boldsymbol{u}_k^T R \boldsymbol{u}_k) + \boldsymbol{\mu}_{k+1}^T (A\boldsymbol{x}_k + E\boldsymbol{u}_k + F) \tag{29}$$

Where $\boldsymbol{\mu}_k$ is the adjoint vector. The adjoint vector recursive equation is:

$$\boldsymbol{\mu}_k = \frac{\partial H_k}{\partial \boldsymbol{x}_k} = \alpha^k Q \boldsymbol{x}_k + A^T \boldsymbol{\mu}_{k+1} \tag{30}$$

The stationary condition is:

$$0 = \frac{\partial H_k}{\partial \boldsymbol{u}_k} = \alpha^k R \boldsymbol{u}_k + E^T \boldsymbol{\mu}_{k+1} \tag{31}$$

According to 31,

$$\boldsymbol{u}_k = -\alpha^{-k} R^{-1} E^T \boldsymbol{\mu}_{k+1} \tag{32}$$

The Hamiltonian system is obtained by combining Equations (26), (31) and (32):

$$\begin{bmatrix} \boldsymbol{x}_{k+1} \\ \boldsymbol{\mu}_k \end{bmatrix} = \begin{bmatrix} A & -\alpha^{-k} E R^{-1} E^T \\ \alpha^k Q & A^T \end{bmatrix} \begin{bmatrix} \boldsymbol{x}_k \\ \boldsymbol{\mu}_{k+1} \end{bmatrix} + \begin{bmatrix} F \\ 0 \end{bmatrix} \tag{33}$$

DOI: 10.13009/EUCASS2017-321

It is assumed that $\boldsymbol{\mu}_k$ is as follows:

$$\boldsymbol{\mu}_k = \alpha^k (P_k \boldsymbol{x}_k - \boldsymbol{v}_k) \tag{34}$$

Replacing (34) in the first equation of (33) gives:

$$\boldsymbol{x}_{k+1} = (Id + \alpha E R^{-1} E^T P_{k+1})^{-1} A \boldsymbol{x}_k + (Id + \alpha E R^{-1} E^T P_{k+1})^{-1} [\alpha E R^{-1} E^T \boldsymbol{v}_{k+1} + F] \tag{35}$$

Replacing (34) and (35) in the second equation of 33 gives:

$$\begin{aligned}&[-P_k + Q + \alpha A^T P_{k+1} (Id + \alpha E R^{-1} E^T P_{k+1})^{-1} A] \boldsymbol{x}_k + [\alpha A^T P_{k+1} (Id + \alpha E R^{-1} E^T P_{k+1})^{-1} \alpha E R^{-1} E^T \boldsymbol{v}_{k+1} \\ &+ \alpha A^T P_{k+1} (Id + \alpha E R^{-1} E^T P_{k+1})^{-1} F + \boldsymbol{v}_k - \alpha A^T \boldsymbol{v}_{k+1}] = 0\end{aligned} \tag{36}$$

This equation must hold for all state sequences $\boldsymbol{x}_k$ given any $\boldsymbol{x}_0$, so that the bracketed terms must individually vanish. Using the matrix inversion lemma,

$$P_k = Q + \alpha A^T [P_{k+1} - \alpha P_{k+1} E (\alpha E^T P_{k+1} E + R)^{-1} E^T P_{k+1}] A \tag{37}$$

and

$$\boldsymbol{v}_k = \alpha A^T \boldsymbol{v}_{k+1} - \alpha A^T P_{k+1} (Id + \alpha E R^{-1} E^T P_{k+1})^{-1} \alpha E R^{-1} E^T \boldsymbol{v}_{k+1} - \alpha A^T P_{k+1} (Id + \alpha E R^{-1} E^T P_{k+1})^{-1} F \tag{38}$$

The infinite horizon solution P and $\boldsymbol{v}$ of the associated discrete time Riccati equation are:

$$P = Q + \alpha A^T [P - \alpha P E (\alpha E^T P E + R)^{-1} E^T P] A \tag{39}$$

and

$$\boldsymbol{v} = \alpha A^T \boldsymbol{v} - \alpha A^T P (Id + \alpha E R^{-1} E^T P)^{-1} (\alpha E R^{-1} E^T \boldsymbol{v} + F) \tag{40}$$

$$\boldsymbol{v} = \alpha A^T (Id + \alpha P E R^{-1} E^T)^{-1} (\boldsymbol{v} - P F) \tag{41}$$

Finally from equations (32), (34) and (26) with $P_{k+1} = P$ and $v_{k+1} = v$:

$$\boldsymbol{u}_k = -\alpha (R + \alpha E^T P E)^{-1} E^T P A \boldsymbol{x}_k - \alpha (R + \alpha E^T P E)^{-1} E^T [P F - \boldsymbol{v}] \tag{42}$$

Note, by defining $\overline{A} = \sqrt{\alpha} A$ and $\overline{E} = \sqrt{\alpha} E$,

$$P = Q - \overline{A}^T P \overline{E} [\overline{E}^T P \overline{E} + R]^{-1} \overline{E}^T P \overline{A} + \overline{A}^T P \overline{A} \tag{43}$$

(43) correspond to the classical Riccati equation apply to the pair $(\overline{A}, \overline{E})$. ∎

Thus, based on the theorem, the faulty controller for the engine is:

$$\boldsymbol{u}_k = \left[f(-K_1.\widehat{\boldsymbol{x}}_k + v^1, S_{doublet}, A_k) \qquad f(-K_2.\widehat{\boldsymbol{x}}_k + v^2, S_{3211}, A_k) \qquad f(-K_2.\widehat{\boldsymbol{x}}_k + v^3, -S_{3211}, A_k) \right]^T \tag{44}$$

Off-line, the gain K and the additional term $\boldsymbol{v}$ are calculated for different values of b_0^1 and b_1^1. In fact, to calculate K and $\boldsymbol{v}$, the Riccati equation have to be solved and it depends on the fault parameters b_0^1 and b_1^1. To avoid a long computational time on-line, these values are interpolated following the estimation of b_0^1 and b_1^1.

4.2 Controller selection

The selection of the controller is performed by minimizing a cost expectation. As shown in Fig. 5, for the controller selection, it is assumed that the controller is changed at the first step or not at all. With respect to Fig. 1, the inputs of the controller selection module are not only mode probabilities but also state and fault parameters estimations.
The cost expectation is calculated on-line in two steps; first the cost is calculated with the predicted state over an horizon H, then for the rest of the mission, an expected cost, calculated off-line, is added.

DOI: 10.13009/EUCASS2017-321

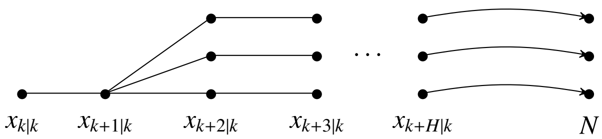

Figure 5: Search space

4.2.1 Prediction of the cost over a short horizon

At each step, $\widehat{\boldsymbol{b}_{\mathbf{0}}}_{k|k}$ and $\widehat{\boldsymbol{b}_{\mathbf{1}}}_{k|k}$ are used to predict the state over a finite horizon H. Three costs are calculated on-line, one cost for each controller.

$$I_k^{k+H}(a) = \sum_{k'=1}^{H} \alpha^{k+k'} (\boldsymbol{x}_{k+k'|k}(a)^T Q_{lqr} \boldsymbol{x}_{k+k'|k}(a) + \boldsymbol{u}_{k+k'}(a)^T R_{lqr} \boldsymbol{u}_{k+k'}(a)) \tag{45}$$

Where a indicates the controller for which the cost is computed.
Moreover, the covariance $P_{k+H|k+H}$ is calculated in order to update the mode probabilities $b_{k+H|k+H}$.

4.2.2 Terminal cost and penalty

Once the model is predict over the horizon H, an expected cost is added for the rest of the simulation.
The cost function is calculated numerically with the indicator of performance off-line. Moreover a penalty of changing of controller is added in order to not change controller without reason:

$$R_{\mu(k+H)}(c, m, a) = J_{k+H}^N(m, a) + P(c, a) \tag{46}$$

Where c is the current controller and $P(c, a)$ correspond to an arbitrary penalty; $P(c_i, a_i) = 0$ and $P(c_i, a_j) = 0.1, \forall i \neq j$

4.2.3 Optimization

The problem to be solved is the following:

$$\min_{a \in A} [\sum_m b_{k+H|k+H}(m) R_{\mu(k+H)}(m, a) + I_k^{k+H}(a)] \tag{47}$$

The action $\widehat{a}$ solving 47 is selected.

5. SIMULATION

5.1 Model and Scenario

The matrices A, B, and C are linearised for an airspeed of $20m/s$ and a slope of $-3°$. The system is discretised with a sampling period Δt of $0.1s$ and the reconfiguration loop have a sampling period Δt_{reconf} of $1s$.
Parameters used for the discounted LQR are as follows.

- $Q_{lqr} = diag\{0, 0, 0, tan^2(\gamma), 1, 0, 0, 0, 0\}$
- $R_{lqr} = 0.1Id_3$
- $\alpha = 0.999$

Parameters used for the Kalman filter are as follows.

- $Q^x = 0.01^2.\Delta t.Id_{9,9}$
- $Q^b = 0.001^2.\Delta t.Id_{5,5}$
- $R = diag\{e^{-2}, e^{-2}, (\frac{0.05\pi}{180})^2, e^{-2}, e^{-2}, (\frac{0.05\pi}{180})^2, e^{-6}, e^{-6}, (\frac{0.05\pi}{180})^2, (\frac{0.05\pi}{180})^2, e^{-2}, e^{-2}\}$

The values in Q_k^b are lower than those of Q_k^x because changes of fault parameters are less likely than perturbation of the evolution model. The values of R_k are taken following the sensor accuracy.
The transition matrix T_M is:

$$T_M = \begin{bmatrix} 1-10^{-7}-2.10^{-8} & 10^{-9} & 10^{-9} & 10^{-9} \\ 10^{-7} & 1-10^{-9}-2.10^{-17} & 10^{-16} & 10^{-16} \\ 10^{-8} & 10^{-17} & 1-10^{-9}-10^{-16}-10^{-17} & 10^{-17} \\ 10^{-8} & 10^{-17} & 10^{-17} & 1-10^{-9}-10^{-16}-10^{-17} \end{bmatrix}$$

The scenario is shown in Table 4. Between $10s$ and $30s$ the engine is locked at 0.2. Between $30s$ and 50 the actuator recovered its performance. Between $50s$ and $70s$, the engine is reduced of 50%. At $70s$ it recovered its performance. At $90s$, the left elevon is locked at its trimmed position.

Table 4: Fault scenario

Time	Mode
$0s$	Nominal
$10s$	Engine locked at 0.2
$30s$	Nominal
$50s$	Engine reduced of 50%
$70s$	Nominal
$90s$	Left elevon locked at trimmed position

5.2 Results

The simulation is done on a scenario of $100s$. The computation time of the method on *Matlab R2014b* is $7s$.

5.2.1 Estimation of state and fault parameters

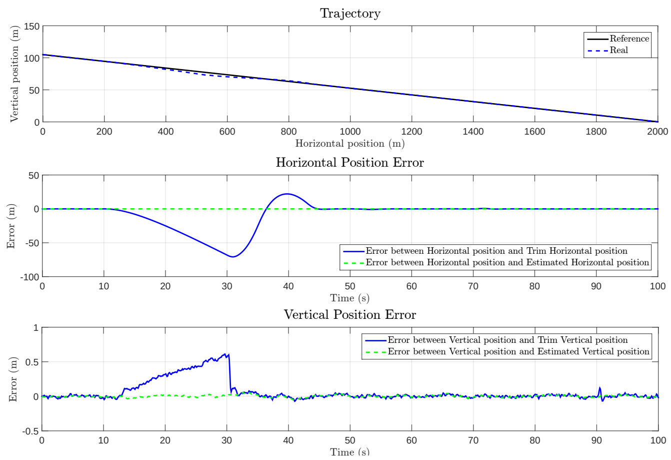

Figure 6: Trajectory

The state estimation errors for horizontal and vertical positions presented by dashed curves in the middle and lower parts of Fig. 6 are small.
Fig. 7 and Fig. 8 show that the estimator estimates well the fault parameters.
The reset of the variance, when the residuals exceed the threshold (see Fig. 9), occurs at relevant times.

5.2.2 Probabilities and action

The mode probabilities are shown in the Fig. 10. The probability of the most likely mode is close to one, except for a short time during the transition. The detection time of faults is fast (less than $3s$). The detection of the thrust recovery is a little longer ($8s$ and $6s$).

DOI: 10.13009/EUCASS2017-321

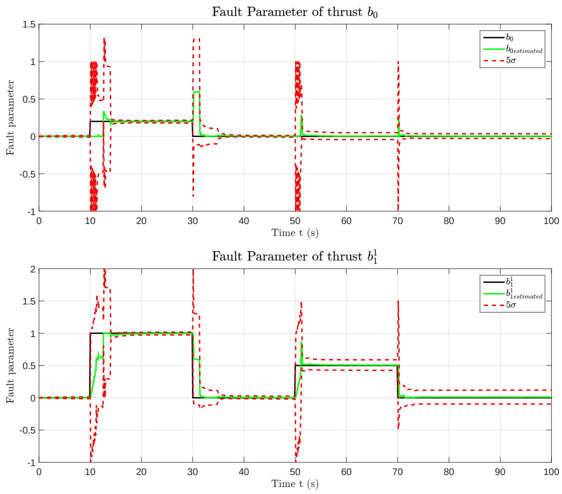

Figure 7: b_0 and b_1 associated to thrust

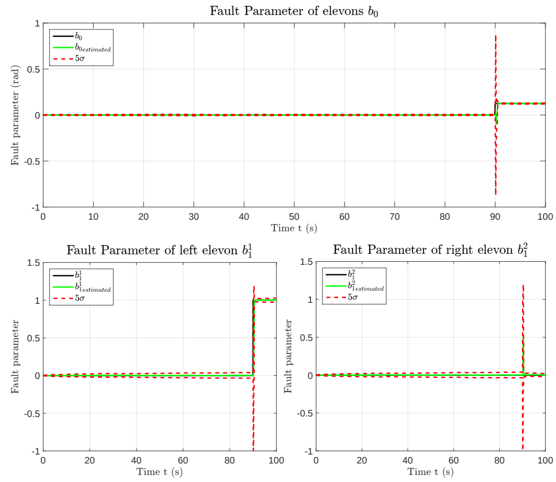

Figure 8: b_0 and b_1 associated to elevons

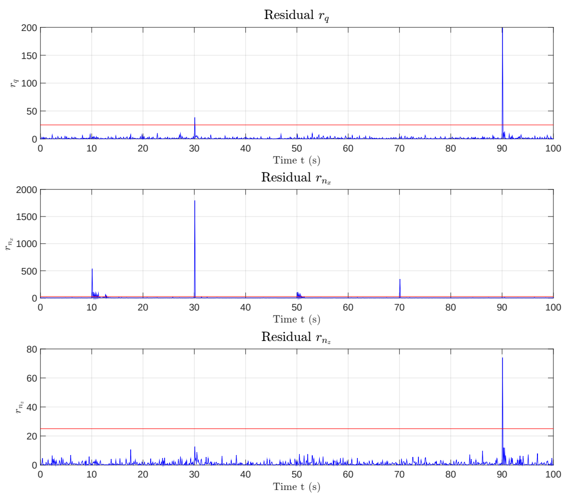

Figure 9: Residuals and thresholds

The controllers are switched as follows. At $11s$, the controller designed for thrust fault is selected even if the thrust fault is not yet detected (at $13s$ as seen in Fig. 10). Indeed, the selection of the controller is based on the mode probabilities but also on a predictive model which depends on the fault parameters. When the engine is detected faulty, the controller is changed at the next step ($12s$).
When the effectiveness of the engine is back, the controller is not changed from c_1 to c_0 because the expected reward is not large enough compared to the penalty associated to any change of controller. Indeed, in nominal mode, the difference of performance between c_1 and c_0 is small.
When the locking case of the left elevon is detected, the controller is switched immediately ($91s$). Indeed the effectiveness of the faulty controller designed for elevons c_2, in the case of elevon faults is higher than the one designed for thrust fault c_1.

5.2.3 Control

Fig. 12 presents the control for the three actuators. Note that the curves represent the differences between actual inputs and trim inputs. When the engine is locked at 0.2 between 10 and $30s$ the difference with its trim value is about -0.08. The UAV fly slower than in nominal case and a slightly positive control is produced for the elevons. When the engine is nominal again, the controller produces a value larger than the trim for the engine and, as the speed increases, it gives for the elevons a value more and more negative. The effect of the loss of effectiveness of the engine between $50s$ and $70s$ is compensated by an increase of its control.

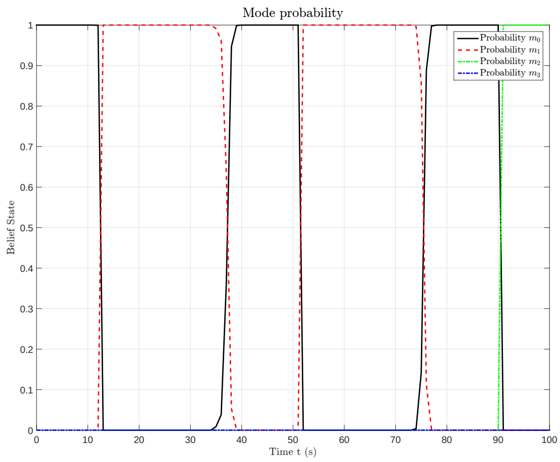

Figure 10: Mode probabilities

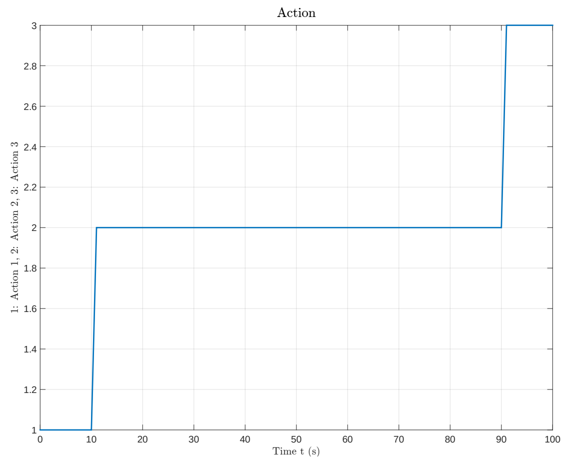

Figure 11: Action: 1 nominal controller, 2 thrust faulty controller, 3 elevons faulty controller

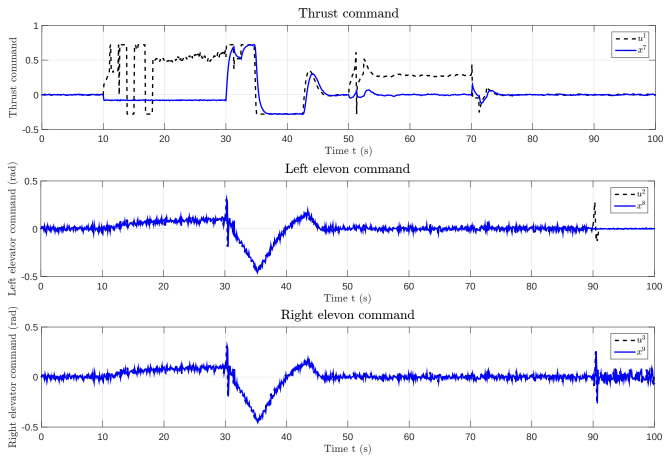

Figure 12: Command for the three actuators

Note that the additional signal $S_{doublet}$ is sent six times when the covariance of associated fault parameters are reset. It is sent three time when the engine is locked -at $10s$, $12.6s$ and $15.6s$- once when the engine is nominal at $30s$, once when the engine is less efficient at $50s$ and once when the engine is nominal at $70s$. The additional signal S_{3211} is sent only one time, at $90s$.

5.2.4 Tracking the reference

The plain curves in the middle and lower part of Fig. 6 present the tracking error for horizontal position and vertical position. The errors are most of the time close to zero, indicating that despite the presence of faults the system state follows the reference leading to an acceptable performance.
When the engine is locked at 0.2, a tracking error appear and the controller cannot reduced this error. It induced a temporary reference tracking error for horizontal and vertical positions. Nevertheless, the tracking of the geometrical trajectory is quite good: the UAV is late but almost on the desired slope γ. This behaviour is the result of the choice for Q_{lqr}. When the engine recover its performance, the recovery time is of $15s$.

6. CONCLUSIONS

In this work, a FTC scheme combining continuous and discrete frameworks has been improved in order to address issues raised by its use for multiple actuator faults on UAV. The first issue is the fact that the UAV engine is a non-redundant actuator and is solved by proposing a LQR controller design considering a discounted cost and a bias in the

DOI: 10.13009/EUCASS2017-321

state equation in order to lead to acceptable performance. The second issue is the slow dynamic of the engine and is solved by selecting the controller to use not only on the basis of mode probabilities and costs associated to modes and controllers but also on the basis of the prediction of the performance of each controller on a rolling horizon using the full dynamics of the UAV. Finally, the third issue is the low observability of fault parameters and the need of reseting their estimated variance and generating excitation signals at appropriate times. This issue is solved by proposing an analysis of the signature of residuals that determines at each time step which variance has to be reset and which excitation signal has to be generated. The method has been applied to a longitudinal model of Altimum 4 taking into account actuator dynamics on a landing approach scenario with actuators becoming faulty at different times. Simulation results indicate that the proposed improvements solve the issues efficiently.
In order to apply the FTC method to the real system two topics shall be addressed. First, the reconfiguration for sensor faults shall be designed and integrated in the proposed FTC method. With possible faults of actuators and sensors the issue of low observability of fault parameters is likely to be more complex that with only possible actuator faults. Investigating the generalized likelihood ratio test[7] may lead to improve the analysis of the signature of residuals. Second the FTC method should be applied to a more complete model; first, with a linearised model of longitudinal and lateral dynamics, then with a non-linear model of UAV. Taking into account directly the non-linear model would imply the use of more sophisticated methods which have to be investigated.

References

[1] Dimitri P Bertsekas, Dimitri P Bertsekas, Dimitri P Bertsekas, and Dimitri P Bertsekas. *Dynamic programming and optimal control*, volume 1. Athena Scientific Belmont, MA, 1995.

[2] Adèle Boche, Jean-Loup Farges, and Henry De Plinval. Reconfiguration control method for multiple actuator faults on UAV. Accepted at IFAC 2017 World Congress.

[3] Adèle Boche, Jean-Loup Farges, and Henry De Plinval. A continuous and discrete framework for reconfiguration of control of faulty systems. In *Computational Intelligence (SSCI), 2016 IEEE Symposium Series on*, pages 1–8. IEEE, 2016.

[4] Inseok Hwang, Sungwan Kim, Youdan Kim, and Chze Eng Seah. A survey of fault detection, isolation, and reconfiguration methods. *IEEE Transactions on Control Systems Technology*, 18(3):636–653, 2010.

[5] Jin Jiang and Xiang Yu. Fault-tolerant control systems: A comparative study between active and passive approaches. *Annual Reviews in control*, 36(1):60–72, 2012.

[6] Jeremy Lesprier, Jean-Marc Biannic, and Clément Roos. Modeling and robust nonlinear control of a fixed-wing uav. In *Control Applications (CCA), 2015 IEEE Conference on*, pages 1334–1339. IEEE, 2015.

[7] Hai Liu and Maiying Zhong. A nonlinear version of the generalized likelihood ratio test. In *Control Conference (CCC), 2014 33rd Chinese*, pages 3175–3180. IEEE, 2014.

[8] Jitendra R Raol, Gopalrathnam Girija, and Jatinder Singh. *Modelling and parameter estimation of dynamic systems*, volume 65. Iet, 2004.

[9] Vincent Sircoulomb, Ghaleb Hoblos, Houcine Chafouk, and José Ragot. Analyse et comparaison de techniques d'estimation d'état sous contraintes inégalité non linéaires. In *5ème Conférence Internationale Francophone d'Automatique, CIFA'2008*, page CDROM, 2008.

[10] Youmin Zhang and Jin Jiang. Integrated active fault-tolerant control using imm approach. *IEEE Transactions on aerospace and electronic systems*, 37(4):1221–1235, 2001.

[11] Youmin Zhang and Jin Jiang. Active fault-tolerant control system against partial actuator failures. *IEE proceedings-Control Theory and applications*, 149(1):95–104, 2002.

[12] Youmin Zhang and Jin Jiang. Bibliographical review on reconfigurable fault-tolerant control systems. *Annual reviews in control*, 32(2):229–252, 2008.